

a L'aerodynamique," *L'Onde Electrique*, Vol. 48, March 1968, pp. 223-225.

<sup>5</sup> Siebert, L. D. and Geister, D. E., "Pulsed Holographic Interferometry vs Schlieren Photography," *AIAA Journal*, Vol. 6, No. 11, Nov. 1968, pp. 2194-2195.

## Generalized Stiffness Matrix of a Curved-Beam Element

HWA-PING LEE\*

NASA Goddard Space Flight Center, Greenbelt, Md.

A CURVED-BEAM is a basic structural element; it represents many engineering structures either to be used alone or contained in a system with structural members of other elementary forms. When such a curved-beam element is employed in a space frame, the loads exerted at the nodes, i.e., the end points, are three-dimensional in the most general case. The stiffness matrix, which relates the forces to the displacements, is of the order of  $12 \times 12$ , because six general nodal forces exist at each node. The nodal forces comprise three rectilinear force components  $F_x$ ,  $F_y$ , and  $F_z$ , one torsional moment  $M_x$ , and two bending moments  $M_y$  and  $M_z$ , among which  $F_x$ ,  $F_y$ , and  $M_x$  are of the in-plane force components that lie in the plane containing the curved-beam element, and the remainders  $F_z$ ,  $M_z$ , and  $M_y$  are of the normal-to-plane force components that produce, at any cross section of the curved-beam, the twisting and bending moments. It is a known fact that a stiffness matrix of a structure may be composed by constituent submatrices. The stiffness matrix of the in-plane force components is readily available,<sup>1,2</sup> but that of the normal-to-plane force components is not seen to exist in an explicit closed form. To find the generalized stiffness matrix of a curved-beam element is, therefore, reduced to seeking that submatrix of the force components of the second group. It is the purpose of this Note to present the generalized stiffness matrix with emphasis on the derivation of the stiffness matrix of the noncoupled normal-to-plane loads. The result may serve as a supplement to the subject matter treated in Ref. 2. Such a generalized stiffness matrix is of practical engineering importance, because it is a requisite to have a precise stiffness matrix when dynamic responses or internal forces of a structural system are sought. Furthermore, the closed form expressions can expedite hand calculation, especially for those who are unable to gain easy access to a digital computer to perform a matrix inversion.

A curved-beam element of uniform cross section is considered. Notations as well as directions of positive nodal forces and displacements are taken as shown in Fig. 1. Force vectors are represented by arrows, and moment vectors are represented according to the right-handed screw rule by a double arrowhead. The flexural stiffness calculated for a traverse cross section is represented by  $EI_y$ , and the torsional stiffness by  $GJ$ .

The derivation will proceed to obtain the flexibility matrix for the curved-beam element subjected to the set of normal-to-plane nodal forces at the left end with the right end being clamped. The corresponding displacements will be determined by introducing the strain energy  $U_n$  expressed in terms of the nodal forces, and then applying Castigliano's second theorem. When cross-sectional dimensions are taken as small compared with  $R$ , the total strain energy takes the form<sup>3</sup>

$$U_n = \frac{R}{2} \left( \int_0^\beta \frac{M^2}{EI_y} d\alpha + \int_0^\beta \frac{T^2}{GJ} d\alpha \right)$$

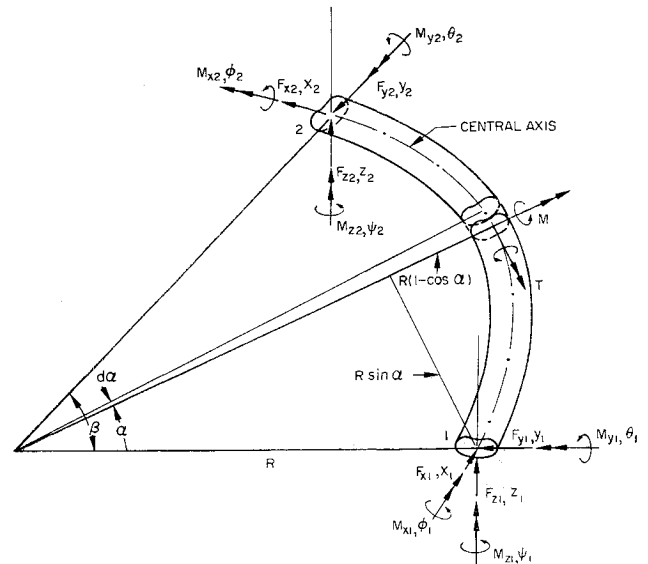


Fig. 1 Nodal forces and displacements relevant to a curved-beam element.

where the bending moment  $M$  and twisting moment  $T$  may be expressed as

$$M = -F_{z1}R \sin \alpha + M_{x1} \sin \alpha - M_{z1} \cos \alpha \quad (1)$$

and

$$T = -F_{x1}R(1 - \cos \alpha) - M_{x1} \cos \alpha - M_{z1} \sin \alpha \quad (2)$$

Applying Castigliano's theorem gives the displacements at node 1 as

$$Z_1 = \frac{\partial U_n}{\partial F_{z1}} = \frac{R}{EI_y} \int_0^\beta M \frac{\partial M}{\partial F_{z1}} d\alpha + \frac{R}{GJ} \int_0^\beta T \frac{\partial T}{\partial F_{z1}} d\alpha$$

$$\phi_1 = \frac{\partial U_n}{\partial M_{x1}} = \frac{R}{EI_y} \int_0^\beta M \frac{\partial M}{\partial M_{x1}} d\alpha + \frac{R}{GJ} \int_0^\beta T \frac{\partial T}{\partial M_{x1}} d\alpha$$

$$\theta_1 = \frac{\partial U_n}{\partial M_{y1}} = \frac{R}{EI_y} \int_0^\beta M \frac{\partial M}{\partial M_{y1}} d\alpha + \frac{R}{GJ} \int_0^\beta T \frac{\partial T}{\partial M_{y1}} d\alpha$$

Carrying out the calculations with the aid of Eqs. (1) and (2) and then collecting terms into a single matrix equation give

$$\begin{Bmatrix} Z_1 \\ \phi_1 \\ \theta_1 \end{Bmatrix} = \frac{R^3}{EI_y} \begin{bmatrix} (\rho f + a) & (\rho d - a) \frac{1}{R} & (\rho e + b) \frac{1}{R} \\ (\rho d - a) \frac{1}{R} & (\rho c + a) \frac{1}{R^2} & (\rho - 1) \frac{b}{R^2} \\ (\rho e + b) \frac{1}{R} & (\rho - 1) \frac{b}{R^2} & (\rho a + c) \frac{1}{R^2} \end{bmatrix} \begin{Bmatrix} F_{z1} \\ M_{x1} \\ M_{y1} \end{Bmatrix}$$

$$\begin{Bmatrix} F_{z1} \\ M_{x1} \\ M_{y1} \end{Bmatrix} = \frac{R^3}{EI_y} [\eta] \begin{Bmatrix} F_{z1} \\ M_{x1} \\ M_{y1} \end{Bmatrix}$$

where a ratio  $\rho = EI_y/GJ$  has been incorporated, and the constants are defined as

$$\begin{aligned} a &= \frac{1}{2} (\beta - \sin \beta \cos \beta) & d &= \sin \beta - c \\ b &= \frac{1}{2} \sin^2 \beta & e &= 1 - \cos \beta - b \\ c &= \frac{1}{2} (\beta + \sin \beta \cos \beta) & f &= \beta - 2 \sin \beta + c \end{aligned}$$

Inverting the flexibility matrix  $[\eta]$ , which satisfies the reciprocal theorem, enables the nodal forces to be expressed in

Received June 6, 1969.

\* Aerospace Technologist, Space Simulation Research Section. Member AIAA.

terms of the nodal displacements under the imposed boundary conditions. Mathematically, it is

$$\begin{Bmatrix} F_{x1} \\ M_{x1} \\ M_{y1} \end{Bmatrix} = \frac{EI_y}{R^3} [\eta]^{-1} \begin{Bmatrix} Z_1 \\ \phi_1 \\ \theta_1 \end{Bmatrix} = [K_{11}^n] \begin{Bmatrix} Z_1 \\ \phi_1 \\ \theta_1 \end{Bmatrix} \quad (3)$$

The corresponding matrices are self-evident, and the inverse of  $[\eta]$  is a symmetric array of elements represented by

$$[\eta]^{-1} = \frac{\text{adj } \eta}{\det \eta} = \frac{1}{|\eta|} \begin{bmatrix} \eta_{11} & -\eta_{12} & \eta_{13} \\ -\eta_{12} & \eta_{22} & -\eta_{23} \\ \eta_{13} & -\eta_{23} & \eta_{33} \end{bmatrix}$$

An analytic inversion of  $[\eta]$  was determined by calculating the co-factors and the determinant. The final results are as follows

$$\begin{aligned} \eta_{11} &= (1/2R^4) \left[ \frac{1}{2}(1 + \rho^2)(\beta^2 - \sin^2\beta) + \rho(\beta^2 + \sin^2\beta) \right] \\ \eta_{12} &= (1/4R^3) [(\beta^2 - \sin^2\beta) + 2\rho\beta(\beta - \sin\beta) + \\ &\quad \rho^2\{\beta(\beta - 2\sin\beta) + \sin^2\beta\}] \\ \eta_{13} &= [\rho(1 - \cos\beta)/2R^3] [(\beta + \sin\beta) + \rho(\beta - \sin\beta)] \\ \eta_{22} &= (1/R^2) \left[ \frac{1}{4}(\beta^2 - \sin^2\beta) + \rho\{\beta^2 - (\beta/2)\sin\beta(2 - \right. \\ &\quad \left. \cos\beta) - \frac{1}{2}\sin^2\beta\} + \rho^2\{\frac{3}{4}\beta^2 - (\beta/2)\sin\beta(2 + \right. \\ &\quad \left. \cos\beta) + \frac{1}{4}\sin^2\beta + 2\cos\beta - 2\} \right] \\ \eta_{23} &= [\rho(1 - \cos\beta)/2R^2] [(\sin\beta - \beta\cos\beta) + \\ &\quad \rho\{\beta(2 + \cos\beta) - 3\sin\beta\}] \\ \eta_{33} &= (\rho/2R^2) [\beta(\beta - \sin\beta\cos\beta) + \rho(\beta^2 + \\ &\quad \beta\sin\beta\cos\beta - 2\sin^2\beta)] \end{aligned}$$

and

$$\begin{aligned} |\eta| &= (\rho/R^4) [(\beta/4)(\beta^2 - \sin^2\beta) + \\ &\quad \rho\{\beta(\frac{1}{2}\sin^2\beta + \cos\beta - 1) - \sin\beta(1 - \\ &\quad \cos\beta) + \beta^3/2\} + \rho^2\{\sin\beta(1 - \cos\beta) - \\ &\quad \beta(\frac{1}{4}\sin^2\beta - \cos\beta + 1) + \beta^3/4\}] \end{aligned}$$

The forces at node 2 can be formed by imposing equilibrium conditions. The applicable equations may be written as

$$\begin{aligned} F_{x1} + F_{x2} &= 0 \\ F_{x1}R\sin\beta - M_{x1}\sin\beta + M_{y1}\cos\beta + M_{y2} &= 0 \\ F_{x1}R(1 - \cos\beta) + M_{x1}\cos\beta + M_{y1}\sin\beta + M_{x2} &= 0 \end{aligned}$$

Expressed in a matrix form, it is

$$\begin{Bmatrix} F_{x2} \\ M_{x2} \\ M_{y2} \end{Bmatrix} = \begin{bmatrix} -1 & 0 & 0 \\ R(\cos\beta - 1) & -\cos\beta & -\sin\beta \\ -R\sin\beta & \sin\beta & -\cos\beta \end{bmatrix} \begin{Bmatrix} F_{x1} \\ M_{x1} \\ M_{y1} \end{Bmatrix} = [\xi] \begin{Bmatrix} F_{x1} \\ M_{x1} \\ M_{y1} \end{Bmatrix} \quad (4)$$

$[\xi]$  represents the transfer matrix relating two sets of force components between nodes 1 and 2. When forces at node 2 are to be expressed in terms of the displacements at node 1, it can be achieved by substituting Eq. (3) in Eq. (4) to yield

$$\begin{Bmatrix} F_{x2} \\ M_{x2} \\ M_{y2} \end{Bmatrix} = [K_{21}^n] \begin{Bmatrix} Z_1 \\ \phi_1 \\ \theta_1 \end{Bmatrix}$$

where

$$[K_{21}^n] = [\xi] [K_{11}^n] = \frac{EI_y}{R^3|\eta|} \begin{bmatrix} \zeta_{11} & \zeta_{12} & \zeta_{13} \\ \zeta_{21} & \zeta_{22} & \zeta_{23} \\ \zeta_{31} & \zeta_{32} & \zeta_{33} \end{bmatrix}$$

and the elements in the above square matrix are

$$\begin{aligned} \zeta_{11} &= -\eta_{11} \quad \zeta_{12} = \eta_{12} \quad \zeta_{13} = -\eta_{13} \\ \zeta_{21} &= -R\eta_{11} + (R\eta_{11} - \eta_{13})\cos\beta + \eta_{12}\sin\beta \\ \zeta_{22} &= -R\eta_{13} + (R\eta_{13} - \eta_{33}) + \eta_{23}\sin\beta \\ \zeta_{23} &= R\eta_{12} + (\eta_{23} - R\eta_{12}) + \cos\beta - \eta_{22}\sin\beta \\ \zeta_{31} &= (\eta_{13} - R\eta_{11})\sin\beta + \eta_{12}\cos\beta \\ \zeta_{32} &= (\eta_{33} - R\eta_{13})\sin\beta + \eta_{23}\cos\beta \\ \zeta_{33} &= (\eta_{23} + R\eta_{12})\sin\beta - \eta_{22}\cos\beta \end{aligned}$$

By reasoning paralleling that in obtaining  $[K_{12}]$  and  $[K_{22}]$  of the in-plane forces as discussed in Ref. 2, the two counterparts in  $[K^n]$ , namely  $[K_{12}^n]$  and  $[K_{22}^n]$ , may be formed by inspection. It leads to that  $[K_{21}^n] = [K_{12}^n]^T$  and  $[K_{22}^n]$  is identical with  $[K_{11}^n]$  except the possible sign changes on the off-diagonal elements. Expressed in terms of the obtained matrix elements, it has

$$[K_{22}^n] = \frac{EI_y}{R^3|\eta|} \begin{bmatrix} \eta_{11} & \eta_{12} & \eta_{13} \\ \eta_{12} & \eta_{22} & \eta_{23} \\ \eta_{13} & \eta_{23} & \eta_{33} \end{bmatrix}$$

Having determined all four submatrices, the stiffness matrix of a curved-beam element for the normal-to-plane forces can be assembled to be

$$\begin{Bmatrix} F_{x1} \\ M_{x1} \\ M_{y1} \\ F_{x2} \\ M_{x2} \\ M_{y2} \end{Bmatrix} = \begin{bmatrix} K_{11}^n & K_{12}^n \\ K_{21}^n & K_{22}^n \end{bmatrix} \begin{Bmatrix} Z_1 \\ \phi_1 \\ \theta_1 \\ Z_2 \\ \phi_2 \\ \theta_2 \end{Bmatrix} = [K^n] \begin{Bmatrix} Z_1 \\ \phi_1 \\ \theta_1 \\ Z_2 \\ \phi_2 \\ \theta_2 \end{Bmatrix} \quad (5)$$

and  $[K^n]$  is seen to be  $6 \times 6$ . The closed form stiffness matrix of a curved-beam element for the in-plane forces is known. Conforming to the notations presently adopted, it may be written as

$$\begin{Bmatrix} F_{x1} \\ F_{y1} \\ M_{x1} \\ F_{x2} \\ F_{y2} \\ M_{x2} \end{Bmatrix} = \begin{bmatrix} K_{11} & K_{12} \\ K_{21} & K_{22} \end{bmatrix} \begin{Bmatrix} X_1 \\ Y_1 \\ \psi_1 \\ X_2 \\ Y_2 \\ \psi_2 \end{Bmatrix} = [K] \begin{Bmatrix} X_1 \\ Y_1 \\ \psi_1 \\ X_2 \\ Y_2 \\ \psi_2 \end{Bmatrix} \quad (6)$$

in which the submatrices  $[K_{11}]$ ,  $[K_{21}] = [K_{12}]^T$ , and  $[K_{22}]$  in explicit form are given in Ref. 2 by Eqs. (5.19), (5.22), and (5.24), respectively.

The generalized stiffness matrix of the curved-beam element can then be obtained by an assemblage of Eqs. (5) and (6). The resulting matrix is of the order of  $12 \times 12$ , and is of the form

$$\begin{Bmatrix} F_{x1} \\ F_{y1} \\ M_{x1} \\ F_{x2} \\ F_{y2} \\ M_{x2} \\ F_{x2} \\ F_{y2} \\ M_{x2} \end{Bmatrix} = \begin{bmatrix} K_{11} & 0 & K_{12} & 0 \\ 0 & K_{11}^n & 0 & K_{12}^n \\ K_{21} & 0 & K_{22} & 0 \\ 0 & K_{21}^n & 0 & K_{22}^n \end{bmatrix} \begin{Bmatrix} X_1 \\ Y_1 \\ \psi_1 \\ Z_1 \\ \phi_1 \\ \theta_1 \\ X_2 \\ Y_2 \\ \psi_2 \\ Z_2 \\ \phi_2 \\ \theta_2 \end{Bmatrix} \quad (7)$$

The forces and displacements in Eq. (7) can be presented in a more tractable form. For instance, the column matrix of the force vectors can be put in the sequence as  $\{F_{x1}, F_{y1}, F_{z1}, M_{x1}, M_{y1}, M_{z1}, F_{x2}, \dots, M_{z2}\}^T$ . The square array of elements in the stiffness matrix must then be rearranged accordingly, but the explicit form is too lengthy to be included. It can be done, however, much more easily when all terms in that stiffness matrix have been numerically evaluated.

### References

- 1 Rasanen, G. K., "Analysis of Curved Bars by the Stiffness Method," M.S. thesis, May 1962, Dept. of Aeronautics and Astronautics, Univ. of Washington.
- 2 Martin, H. C., *Introduction to Matrix Methods of Structural Analysis*, McGraw-Hill, New York, 1966, pp. 144-148.
- 3 Seely, F. B. and Smith, J. O., *Advanced Mechanics of Materials*, 2nd ed., Wiley, New York, 1957, pp. 454-456.

## Generalized Gram-Charlier Method for Curve-Fitting Statistical Data

FRED R. PAYNE\*

The Pennsylvania State University, University Park, Pa.

### Nomenclature

$A_{pq}$	= matrix ( $3 \times 3$ ) of constants [see Eq. (3)]
$B_{ij}$	= matrix ( $3 \times 3$ ) of constants [see Eq. (6)]
$C_{ij}(x_2)$	= matrix ( $3 \times 3$ ) of numbers dependent on $x_2$ [see Eq. (2)]
$C_{ijkl}$	= matrix ( $3 \times 3 \times 3 \times 3$ ) of constants [see Eq. (6)]
$D_{pq}$	= matrix ( $3 \times 3$ ) of constants [see Eq. (5)]
$E$	= square error [see Eq. (7)]
$F_\alpha$	= trial functions [see Eq. (6)]
$M_{ij}(x_2)$	= matrix ( $3 \times 3$ ) of numbers [see Eqs. (4) and (5)]
$r_i$	= three-vector position difference
$R_{ij}$	= covariance tensor [see Eq. (1)]
$R_{\alpha\alpha}$	= diagonal elements of $R_{ij}$ (no sum)
$x_i, x'_i$	= position vectors of measuring probes
$W(r)$	= weight function [see Eq. (7)]
$\varphi(r, x_2)$	= Gaussian distribution [see Eq. (3)]
$\psi(r, x_2)$	= Gaussian distribution [see Eq. (5)]

THE method described below arose from the requirement to fit analytic forms to velocity covariances measured in the turbulent wake of a circular cylinder.<sup>1</sup> The covariance is defined by

$$R_{ij}(\mathbf{r}, x_2) = u_i(\mathbf{x})u_j(\mathbf{x}') \quad (i, j = 1, 2, 3) \quad (1)$$

where  $\mathbf{r} = \mathbf{x}' - \mathbf{x}$  is the three-vector separation of measuring probes located at  $\mathbf{x}$  and  $\mathbf{x}'$ . Grant measured  $R_{ij}$  defined as in Eq. (1) for  $i = j = 1, 2, 3$  for various  $\mathbf{r}, x_2$  values. His measurements generated 49 curves.

Early attempts by the author to fit analytic expressions to the data were based on a series of multidimensional Hermite polynomials, e.g.,

$$R_{ij}(\mathbf{r}, x_2) = C_{ij}(x_2) \sum_{m,n=0}^k \frac{\partial^{m+n}}{\partial r_m \partial r_n} \varphi(\mathbf{r}, x_2) \quad (2)$$

Received February 13, 1969; revision received July 22, 1969. Supported in part by the U.S. Office of Naval Research under Contract Nonr 656(33); taken in part from a Ph.D. thesis in the Department of Aerospace Engineering, The Pennsylvania State University, University Park, September 1966. Partly supported by Internal funding, Fort Worth Division, General Dynamics Corporation.

\* Assistant Professor, Department of Aerospace Engineering; now Design Specialist, Internal Aerodynamics, Fort Worth Division, General Dynamics Corporation, Fort Worth, Texas.

where

$$\varphi(\mathbf{r}, x_2) = \exp[-A_{pq}(x_2)r_p r_q], \quad A_{pq} \geq 0 \quad (3)$$

This scheme attempts to construct a model from the Gaussian distribution  $\varphi$  and its first  $k$  moments.

This approach proved unsatisfactory for the turbulence data. The difficulty was the determination of analytic approximations uniformly valid over a wide range of  $r_i$  separations; to be specific, good matches for small  $r_i$  decayed too rapidly as  $r_i$  increased to the order of half the wake thickness. Increasing the value of  $k$  from 4 to 8 showed, as indicated possible by Cramer,<sup>2</sup> little improvement.

Reconsideration of the physics of turbulent flows suggested a "two-component" model. The reasoning, similar to that of Grant<sup>1</sup> and Townsend,<sup>3</sup> is that the small-scale motions are nearly Gaussian whereas the large-scale motions surely are not. Hence, the model chosen used  $\varphi$  and its derivatives to represent the large eddies and a pure exponential to describe the small eddies, e.g.,

$$R_{ij}(\mathbf{r}, x_2) = C_{ij}(x_2) \sum_{m,n=0}^k \frac{\partial^{m+n}}{\partial r_m \partial r_n} \varphi(\mathbf{r}, x_2) + M_{ij}(x_2) \psi(\mathbf{r}, x_2) \quad (4)$$

where  $\varphi$  is defined by (3), and

$$\psi(\mathbf{r}, x_2) = \exp[-D_{pq}r_p r_q], \quad D_{pq} \geq 0, \quad M_{ij} = 1 - C_{ij} \quad (5)$$

Applying (4) and (5) yielded, for the 49 curves measured by Grant, errors of less than 10% for the first five moments and pointwise errors generally of less than 10%. This is more than adequate due to inherent difficulties in turbulence measurements wherein 10-20% errors are customary.

The largest errors in quantities usually considered significant in turbulent flows occurred in the Taylor microscale, which is closely associated with the curvature at the  $r_i$  origin. This was not a serious fault for the immediate problem of determining large eddy structure, which is detailed elsewhere.<sup>4,5</sup>

For applications in which the Taylor microscale is important, it appears that generalization of  $\psi$  to higher-order Hermitian polynomials is the simplest approach. This is consistent with the idea that  $\psi$  describes the small-scale eddies that determine the Taylor microscale.

A note on computation techniques as used on the IBM 7074 may be useful. The error criterion used to determine the best match, e.g., best values of  $D_{pq}, C_{ij}, A_{pq}$ , was to minimize the integrated square error. Grant's data included only the trace of the correlation tensor, hence  $i = j$ . For computational simplicity the programed forms of (4) and (5) were taken as

$$F_\alpha = C_{\alpha\alpha}(1 + B_{ij}r_i r_j + C_{ijkl}r_i r_j r_k r_l) \exp[-A_{pq}r_p r_q] + (1 - C_{\alpha\alpha}) \exp[-D_{pq}r_p r_q] \quad (6)$$

where  $F_\alpha$  ( $\alpha = 1, 2, 3$ ) is the trial match for  $R_{\alpha\alpha}$  (no sum on repeated Greek indices).

Since Grant's data consisted entirely of  $R_{\alpha\alpha}$  measurements and predominantly of probe separations along the  $r_i$  axes, the form (6) was programed in a considerably simplified version. The  $A_{pq}$  and  $D_{pq}$  were taken to be diagonal tensors. The odd-ordered derivatives of  $\varphi$  were dropped as well as cross derivatives. The basis for these simplifications is the lack of data at separations in more than one  $r_i$  direction. Therefore,  $B_{ij}$  and  $C_{ij}$  also were taken to be diagonal and dependent only on  $x_2$ .

Since Grant found three basic types of correlations, i.e., positive, single zero, and double zero, slightly different programs were used in each case in the initial investigation.<sup>5</sup> Zeroes and/or zero slope points of  $R_{\alpha\alpha}$  were used to reduce computer time. Initial values were picked for  $C_{\alpha\alpha}, A_{ij}$ , and  $D_{ij}$  and automatically varied to minimize the square error  $E$  defined by

$$E = \int_{-\infty}^{\infty} (R_{\alpha\alpha} - F_\alpha)^2 W(r) dr \quad (7)$$